

DETECTION AND MAPPING OF ICE CLOUDS IN MARS' MESOSPHERE E. Sefton-Nash¹, N. A. Teanby¹, S. B. Calcutt², J. Hurley², P. G. J. Irwin². ¹School of Earth Sciences, University of Bristol, U.K. (e.sefton-nash@bristol.ac.uk), ²Atmospheric, Oceanic and Planetary Physics, University of Oxford, Oxford, U.K.

Introduction: Mesospheric clouds have been observed in a variety of infrared, ultraviolet and visible wavelength datasets, but spatial and temporal coverage is often limited because observation strategies are typically driven by surface, rather than atmospheric science. The formation of CO₂ ice clouds in the mesosphere of Mars is expected, since temperature profiles from observations and climate models can drop below the frost point of CO₂.

Analysis of Mars Orbital Camera (MOC) limb-facing images during Mars Years 24-26, produced observations of ~40 mesospheric clouds [1]. These detections were corroborated by spatially and temporally coincident nadir spectra acquired by the Thermal Emission Spectrometer (TES). Results suggested either a water or CO₂-ice composition and a typical altitude range of 60-80 km [1]. Similar conclusions regarding cloud altitude and composition were drawn using data from ESA's HRSC imager and OMEGA imaging spectrometer [2, 3, 4], as well as observations by NASA's THEMIS-VIS imager [5]. Stellar occultation techniques using the SPICAM ultraviolet spectrometer aboard Mars Express yielded reports of subvisible CO₂ ice clouds at around 80-100 km [6].

However, the total geographic and temporal distribution of these features remains unconstrained due to limitations in data coverage. We present new detections of mesospheric clouds using data from NASA's Mars Climate Sounder (MCS) aboard MRO.

Observations: The MCS instrument acquires vertical profiles of limb-spectra in 9 bands [7]. Completing a polar orbit once every 2 hours since 2006, MCS has produced a dataset of global coverage and therefore is ideal for observing temporally sparse and geographically dispersed atmospheric phenomena. We use data from visible band A6 (~0.3-3 μm), in which daytime cloud features appear bright relative to the background. Because the MCS boresight is limb-facing, clouds observed in successive vertical profiles cause loop-shaped structures to appear in the data. The altitude of the tangent point of the line of sight to the cloud gives projected apparent altitude of the cloud at each orbital position. The orbital path of the spacecraft causes the apparent altitude to increase then decrease as the cloud is viewed from below (Fig. 1: Top - 0, 1, 2), edge on (3) and from above (4, 5). This causes a discrete cloud to appear as a continuous loop in the radiance profile, which is acquired along-track. The apex of a loop gives the true altitude of a discrete cloud.

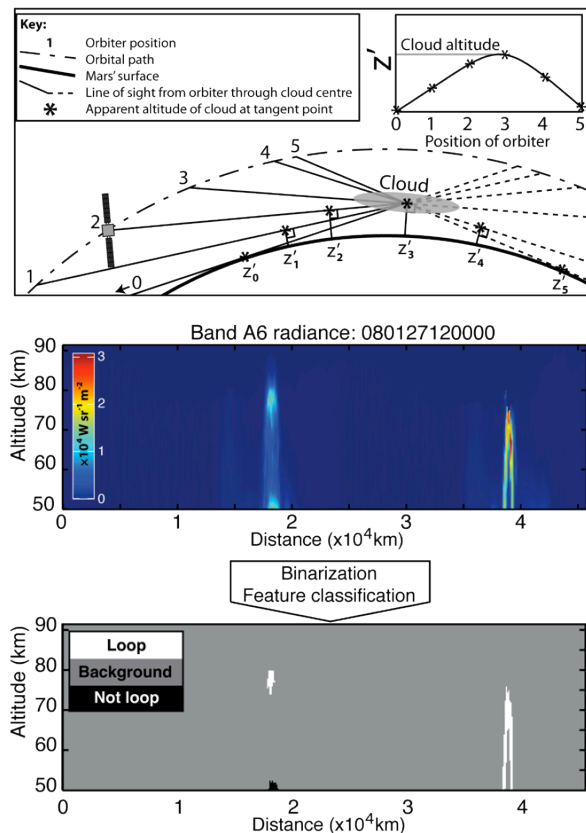


Fig. 1: Top – orbital geometry. Middle – Band A6 radiance showing loop features. Lower – Result of binarization and classification of gridded radiance data to detect loop features.

Methods: Limb spectra were processed and calibrated using the standard pipeline. Spectra were then resampled onto regular grids with 100 km horizontal and 0.5 km vertical spatial resolution. Grids were binarized into object matrices by thresholding using a predefined radiance of $6 \times 10^4 \text{ W sr}^{-1} \text{ m}^{-2}$ (Fig. 1). The detection of loop features was performed using automated object analysis. Features were classified as loops if they were above 50 km altitude, had a cross-sectional area between 750-22,500 km², had major axes orientations within 10° of vertical and had aspect ratios > 2 . The along-track geographic spacing of spectra varies between data products. Artifacts, produced by gridding of sparsely spaced or variably-spaced spectra were found to cause false classifications of features, the algorithm reporting the presence of a loop where there was none. We found spacings of 400 km or less sufficient to resolve loops. 2810 data files that contained spectra spaced more widely than this threshold were not used. A total of 3898 data files acquired between Dec. 2006 (MY 28) and Apr. 2011 (MY 30)

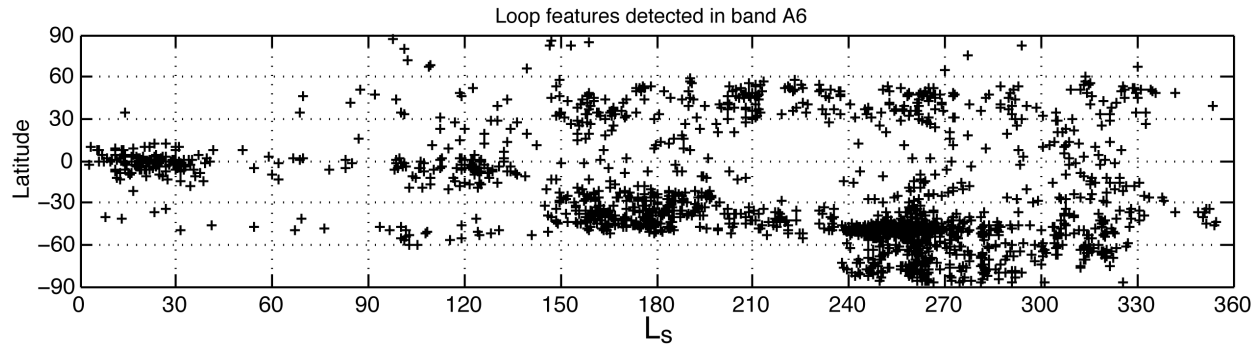


Figure 2: Distribution of features detected in band A6 that were classified as clouds by our algorithm.

were processed and analyzed for detection of loop features.

Results: In Northern hemisphere summer, clouds are detected predominantly at equatorial latitudes, with higher frequency during L_s ranges 0° – 40° and 100° – 130° (Fig. 2). This distribution is not seen during the dust storm season, when we observe a paucity of clouds at equatorial latitudes. Instead, most positive detections tend to occur in two mid-latitude bands ($\sim 30^\circ$ – 60°), with more detections in the Southern Hemisphere, particularly in the periods $L_s = 150^\circ$ – 190° and 240° – 270° . The two regimes are separated a sharp boundary at $L_s = 150^\circ$, which loosely marks the beginning of dust storm season. We plot the geographic distribution in non-dust storm and dust storm conditions (Fig. 3) to highlight the disparity.

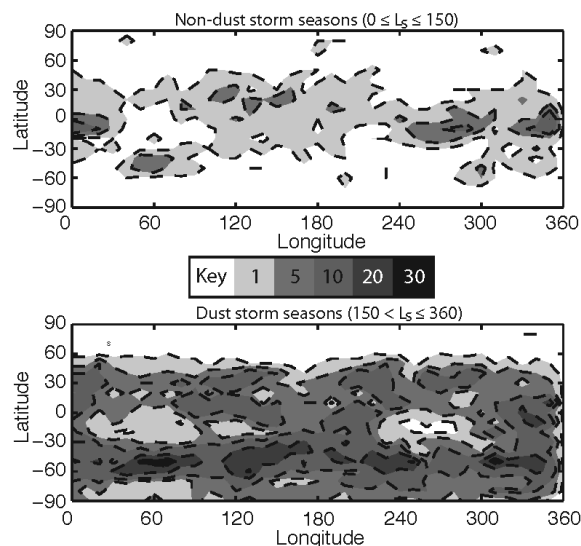


Figure 3: Global distribution of cloud features during Northern hemisphere summer (top) and during Northern hemisphere winter/dust storm season (bottom). Contours are calculated by binning detections into geographic squares of side 10° .

We also ran the detection algorithm on data from mid infrared band A4 (11.49 – $12.20 \mu\text{m}$), which yielded an almost identical spatiotemporal distribution of clouds. We found this to also be true for features detected on the nightside. Reported altitudes of detected mesospheric clouds lie in the range 45 – 110 km [5, 6]. On average we find highest number of clouds at 70 km , although the variation of this value over season and location is under investigation.

Discussion: We find that the distribution we present compares well to previous detections of clouds in Mars' mesosphere [1–6]. In particular we note that cloud formation has little or no longitudinal bias. During N. hemisphere summer cloud formation appears relatively rare, but concentrated almost entirely at equatorial latitudes, while during dust-storm season clouds tend to form along mid-latitude bands and preferentially in the S. hemisphere (Fig. 3). Furthermore, cloud production appears higher during several well-defined time periods during the Martian year (Fig. 2). The formation of CO_2 ice clouds is likely to be predominantly controlled by temperature, but a limiting factor may be the abundance of dust particles available as nucleation sites. Higher cloud abundance during dust storm season is consistent with this theory. To further constrain the cause of cloud formation, our detections will be correlated with the seasonal and spatial distribution of temperatures produced by Mars climate models.

References: [1] Clancy R. T., et al. (2007) *J. Geophys. Res.* 112, E04004. [2] Montmessin F., et al. (2007) *J. Geophys. Res.* 112, E11S90. [3] Scholten, F., et al. (2010) *Plan. Space. Sci.* 58, 1207–1214. [4] Määttänen, A., et al. (2010), *Icarus*, 209, 452–469. [5] McConnochie, T. H., et al. (2010) *Icarus* 210, 545–565. [6] Montmessin F., et al. (2006) *Icarus*, 183, 403–410. [7] McCleese, D. J. et al. (2007), *J. Geophys. Res.* 112, E05S06.